Environmental Science Nano

PAPER

View Article Online
View Journal | View Issue

Cite this: *Environ. Sci.: Nano*, 2019, **6**, 646

An assessment of the dietary bioavailability of silver nanomaterials in rainbow trout using an *ex vivo* gut sac technique†

Nathaniel J. Clark, David Boyle and Richard D. Handy *

The uptake of engineered nanomaterials (ENMs) by the gut of fishes is poorly understood. This study assessed the utility of the *ex vivo* gut sac method for measuring bioavailability following exposures to silver nanoparticles (Ag NPs) or silver sulphide nanoparticles (Ag_2S NPs). Whole gut sacs were prepared from rainbow trout and filled with saline containing control (no added Ag) or 1 mg L^{-1} Ag as $AgNO_3$, Ag NPs or Ag_2S NPs and then incubated for 4 h. The mucosa and muscularis were analysed for total silver concentrations. The amount of Ag associated with the gut ranged from 2% to 20% of the exposure dose, with the majority being associated with the mucosa. For the muscularis in the $AgNO_3$ treatment, the anterior, mid and hind intestine had significantly more Ag (4, 6 and 6 fold higher) compared to the oesophagus and stomach (~75 ng g^{-1} dry weight tissue). For Ag NPs, there was a similar pattern of total Ag concentrations in the mucosa, with proportionally more total Ag in the mid (1506 ± 907 ng g^{-1} dw) and hind (732 ± 258 ng g^{-1} dw) intestine, but not statistically different from the equivalent $AgNO_3$ treatment. For Ag_2S NPs, there were no differences in total Ag by anatomical region, or compared to $AgNO_3$, for the mucosa. Crucially, sometimes the muscularis from the $AgNO_3$ treatment showed much higher Ag concentrations than either NP treatment. Overall, the gut sac method can determine the bioavailability of ENMs. Both NPs were less bioavailable than the metal salt and with no material-type effects.

Received 5th September 2018,
Accepted 19th November 2018

DOI: 10.1039/c8en00981c

rsc.li/es-nano

Environmental significance

Information on bioaccumulation potential is an important requirement of environmental risk assessment. However, the bioaccumulation potential of engineered nanomaterials (ENMs) *via* the gut of fishes is poorly understood and alternative methods are needed to reduce *in vivo* testing. This study showed the utility of a well-established *ex vivo* fish gut sac method for measuring the bioaccumulation potential of silver nanoparticles (Ag NPs) and silver sulphide nanoparticles (Ag_2S NPs). Bioavailability was low, and both types of NPs were less bioavailable than the metal salt, with no material-type effect between the forms of the NPs. The gut sac method could be used in a tiered approach to reduce *in vivo* testing and inform on the fate of ENMs in aquatic food chains.

Introduction

The persistence, bioaccumulation potential and toxicity (PBT) of chemicals are crucial aspects of environmental risk assessment. For engineered nanomaterials (ENMs), fate and behaviour studies are informing on persistence.[1–4] There is also a growing body of literature on ecotoxicity,[5,6] but the bioaccumulation potential of ENMs has received less attention.[7,8] Dissolved silver is regarded as one of the most toxic elements in the periodic table to aquatic species,[9] but less is known about particulate forms of silver in freshwater ecosystems and their bioaccumulation.

Computational models predict that surface waters may contain ng L^{-1} concentrations of Ag from ENMs and that sediments may contain mg kg^{-1} amounts of silver from ENMs.[10] However, while commercial products often contain pristine Ag NPs, this may not be the most relevant form in the environment. A variety of biogeochemical processes may transform or modify ENMs as they are released (for reviews, see ref. 2–4). For example, sulphur will react with silver ENMs during wastewater treatment in an exposure time- and size-dependent manner,[11] with the formation of inert silver sulphide particles. Consequently, it is the latter form that is more persistent in the environment.[3,4] The settling of ENMs from the water column is also a concern because of subsequent exposure of the sediments, associated biofilms and the benthic organisms;[12] with potential for trophic transfer in the case of silver to other organisms in the food web including fishes.

School of Biological and Marine Sciences, University of Plymouth, Plymouth, UK. E-mail: r.handy@plymouth.ac.uk

† Electronic supplementary information (ESI) available. See DOI: 10.1039/c8en00981c

The bioaccumulation potential and effects of dietary exposure to metal salts are well known in freshwater fish (for reviews, see ref. 13 and 14) and the trophic transfer of dissolved forms of silver to fishes has been demonstrated in the laboratory.[15,16] In contrast, the bioaccumulation potential from dietary exposure to ENMs in fish is poorly understood and with insufficient data to reach a consensus on which ENM characteristics will be important to uptake.[8] For some ENMs, the dietary bioavailability to the internal organs seems minimal to fish (single walled carbon nanotubes,[17] TiO_2 [18]), but for other ENMs some bioaccumulation of total metal in the organs may occur (ZnO NPs[19]). For Ag NPs the situation is unclear. One study with trout intestinal cell cultures showed some total Ag associated with the gut cells following exposure to citrate-coated Ag NPs.[20] However, epithelial cell cultures do not have all of the tissue layers of the intact gut, and arguably, the gut sac preparation is much closer to the *in vivo* condition for investigations on bioavailability.

In Europe, the OECD 305 test with fish is required to assess the *in vivo* bioaccumulation potential for all new substances, including ENMs. However, the *in vivo* test is not intended to reveal mechanistic details on bioavailability and the testing strategy has been criticised for not including *in vitro* tiers to identify ENMs of concern and also for not reducing the burden of animal testing (the 3Rs).[8] Some alternative approaches are therefore needed. The gut sac technique is a well-established *ex vivo* method which has been used to measure the apparent accumulation of dissolved metals in the gut tissues of fish (*e.g.* Cu,[21] Fe,[22] Hg,[23] Zn, Cd,[24] and Pb[25]) and has been applied to pristine ENMs (TiO_2,[26]). The technique involves removing the entire gastrointestinal tract (GIT) of a large fish (*e.g.*, 150 g trout), filling the gut lumen with the test substance, and incubating this for a short period before analysing the tissue compartments for the total concentrations of the test substance. The gut sac method can also identify bioavailable fractions of metals and the medium is easily manipulated to study metal speciation effects (*e.g.* Ag,[15]). However, the gut sac technique has not been applied to Ag-containing ENMs in fish.

This study aimed to demonstrate the utility of the gut sac technique in rainbow trout (*Oncorhynchus mykiss*) for determining the bioavailability of total Ag from Ag NPs compared to $AgNO_3$. For the metal salt and any potential Ag dissolution from Ag NPs, the speciation of soluble silver will be influenced by the chloride concentration in the water,[27] and consequently chloride concentration is also a modulating factor involved in branchial uptake of silver by fish,[28] but its effects on the gut are unexplored. Therefore, an additional aim of this study was to investigate Ag accumulation in the gut tissue in the presence and absence of chloride in the medium for both $AgNO_3$ and Ag NP exposures. Silver dissolution from the Ag NPs was also measured in the gut saline used and in the presence of other ligands such as amino acids, and at low pH, to aid the interpretation of the data. Finally, the accumulation of total silver in the gut tissue from exposure to the more environmentally relevant Ag_2S NPs was measured to inform on whether this persistent material would present more hazard than the pristine (unmodified) Ag NPs.

Methodology

Stock animals

Rainbow trout (*Oncorhynchus mykiss*), weighing 212 ± 39 g (mean ± standard deviation, n = 42), were obtained from Exmoor Fisheries. The fish spent 10 days in a semi-static quarantine tank before being moved to a re-circulating system for a further 7 day period to become accustomed to the water quality (dechlorinated Plymouth tap water) and the tank environment (social hierarchy formation). During this period, fish were fed twice a day using a commercial pelleted food. Water quality was checked daily (data are mean ± S.E.M, n = 30) for pH (7.3 ± 0.1), temperature (16.7 ± 0.1 °C), and dissolved oxygen (96.8 ± 0.7 mg L^{-1}). The background total silver concentration of the aquarium water housing the fish over the course of the experiment was below the limit of detection for the ICP-MS (0.1 μg L^{-1}). The commercial feed contained 53.0 ± 2.1 ng g^{-1} dry weight of total Ag (mean ± S.D., n = 3 random batches of pellets). Prior to experiments, fish were unfed for 48 h to aid in evacuation of the gastrointestinal tract content and to facilitate the preparation of the gut sacs.

Preparation and characterization of Ag NPs and $AgNO_3$ solutions

The Ag NPs and Ag_2S NPs were provided by Applied Nanoparticles (Barcelona). The Ag NPs were supplied at (manufacturer's information) a nominal size and concentration of 60 nm and 10.8 g L^{-1}, respectively. The Ag_2S NPs had a nominal size and concentration of 35 nm and 14 g L^{-1}, respectively. The Ag NP material was dispersed in 25 μM tannic acid and 5.5 mM sodium citrate, and the Ag_2S material was dispersed in 1 mg mL^{-1} PVP. Transmission electron microscopy (TEM, JEOL-1200EX II) was conducted at Plymouth to confirm the primary particle diameters of the materials. Briefly, a copper grid was placed on top of a drop of the stock suspension, after which the grid was removed and allowed to dry for 10 min at room temperature before imaging. TEM revealed the primary particle diameter of Ag NPs and Ag_2S NPs to be 55 ± 3 nm (mean ± S.D., n = 120) and 37 ± 19 nm (mean ± S.D., n = 103), respectively (Fig. 1). The concentration of the total Ag in the stocks of Ag NPs and Ag_2S NPs was also measured by inductively coupled plasma mass spectrometry (ICP-MS, Thermo X-series 2 ICP-MS). The stock concentrations for (mean ± S.D., n = 4) the Ag NPs and Ag_2S NPs were 9.9 ± 0.3 and 2.3 ± 0.2 g L^{-1}, respectively. The latter stock was from a bespoke commercial synthesis undergoing validation, and for understanding potential settling in the vials as supplied, emphasis was therefore on the measured, rather than nominal, concentration of silver. Nanoparticle tracking analysis (NTA) was conducted to confirm that the materials could be dispersed adequately from the stocks supplied by the manufacture. Briefly, 1 mg L^{-1}

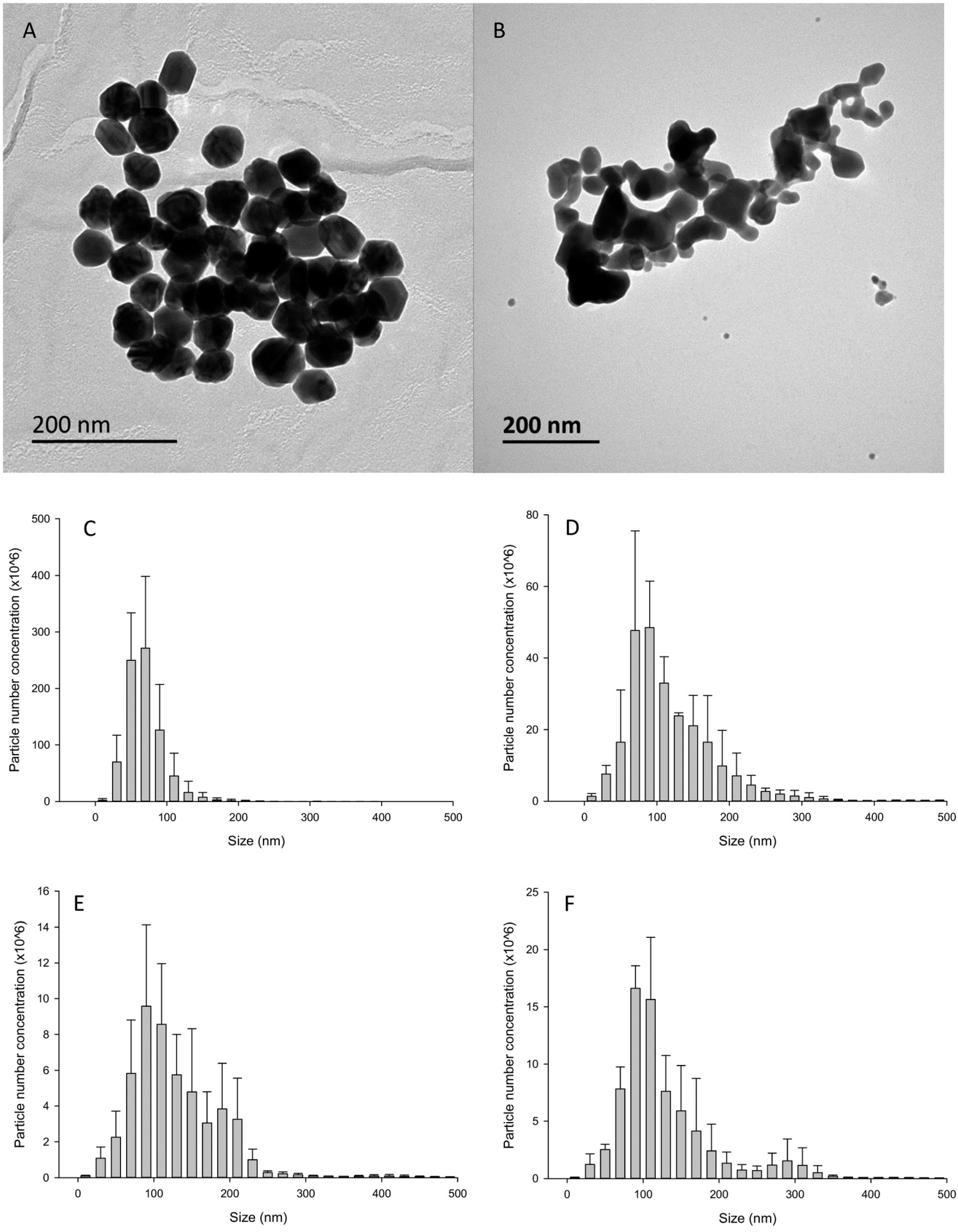

Fig. 1 Transmission electron micrographs of Ag NPs (A) and Ag_2S NPs (B). Particle aggregation behaviour of Ag NPs and Ag_2S NPs in ultrapure water (C and E, respectively) and physiological gut saline (D and F, respectively) measured by NanoSight Tracking Analysis. Note the small percentage of particles above 300 nm in the Ag_2S NP panels only. Mean ± S.D. (n = 3).

dispersions of the Ag NPs were made in ultrapure water by pipetting 100 μL of a secondary stock (1 in 10 dilution from stock solution supplied) and made up to 1 L with ultrapure water, or saline as appropriate. The suspension was then sonicated for 1 h and analysed in triplicate. The mean (± S.D.) hydrodynamic diameter was 66 ± 4 nm (n = 3) for 1 mg L^{-1} Ag NPs and 135 ± 7 nm (n = 3) for 1 mg L^{-1} Ag_2S NPs (Fig. 1). NTA was also conducted in freshly spiked gut saline (see below) to better understand particle behaviour in a biologically relevant medium. As expected, both types of Ag NPs and Ag_2S NPs tended to aggregate in the high ionic strength medium compared to ultrapure water. Dispersions of Ag NPs in the gut saline had a mean hydrodynamic diameter of 115 ± 19 nm (n = 3). For Ag_2S NPs in saline the mean hydrodynamic diameter was 135 ± 13 nm (n = 3). NTA was also conducted after the Ag NPs or Ag_2S NPs had been in the gut saline for 4 h to mimic the behaviour over the duration of the gut sac experiment (kept under the same conditions, see below). The NTA could not detect a significant number of particles after 4 h, indicating that most of the particles had settled from the water column.

Gut sac preparation

Whole gut sacs were prepared according to Handy *et al.*[21] with slight modifications.[29] The technique involved filling the entire gut lumen with the test solution of interest and then isolating the anatomical regions by suturing them closed. Then, the filled gut sacs can then be individually placed in clean serosal (blood side) saline to incubate for 4 h. The apparent metal accumulation in the tissue is then measured. Briefly, fish were euthanized by induced concussion and then pithing (schedule 1 method in accordance with ethical approvals, Home Office, UK, and in compliance with the EU directive 2010/63/EU), and their total weight was recorded. The whole gastrointestinal tract was carefully removed and then the liver and gallbladder were discarded. The whole gut was then separated into anatomical regions of the oesophagus, stomach, anterior intestine with the pyloric caeca, mid intestine and hind intestine. The gut segments were washed with a physiological saline (in mmol L^{-1}: NaCl, 117.5; KCl, 5.7; $NaHCO_3$, 25.0; $NaH_2PO_4{\cdot}H_2O$, 1.2; $CaCl_2$, 2.5; $MgSO_4{\cdot}7H_2O$, 1.2; glucose, 5.0; mannitol, 23.0; pH 7.8) from Handy *et al.*[21] The resulting portions of gut were formed into sacs by closing one end with surgical thread, filled with the gut saline as appropriate and then weighed.

The gut sacs for each anatomical region were inevitably of different sizes, but each gut sac was filled as much as possible with one of four solutions: gut saline (described above, no added Ag) or gut saline spiked with 1 mg L^{-1} Ag as $AgNO_3$, Ag NPs or Ag_2S NPs. The volume of the added saline was recorded to facilitate calculation of the absolute dose in each gut sac (see below). The exposure concentration of 1 mg L^{-1} Ag was selected as a sub-lethal concentration to ensure that any Ag accumulated by the tissue could be readily detected as well as to enable direct comparison with our previous gut sac studies on TiO_2 ENMs. The silver speciation from the $AgNO_3$ in the gut saline above (pristine, no contact with fish tissue) was theoretically calculated using Visual MINTEQ 3.1 by J. P. Gustafsson (https://vminteq.lwr.kth.se/download/). The calculated silver species in the normal gut saline containing chloride was Ag^+, 79.55%; AgCl (aq), 20.21%, and $AgCl_2^-$, 0.22%. For the experiments with chloride-free saline, the relevant salts of chloride-containing chemicals were substituted with equimolar concentrations of $NaNO_3$, KNO_3 and $CaNO_3$ in the recipe above. The calculated silver speciation in the chloride-free saline at pH 7.8 was Ag^+, 96.1% and $AgNO_3$ (aq), 3.91%, indicating that the silver was dissolved. The chloride-free experiment was not performed with the Ag_2S NPs as there was not expected to be an effect due to the inert nature of this material.

Tissue compartments were subsequently closed using suture thread and the tissues were carefully weighed to confirm the net mass of the exposure medium added to each compartment. Tissues were individually incubated in 50 mL (stomach and anterior intestine) or 15 mL (oesophagus, mid and hind intestine) tubes containing 20 and 7.5 mL of the appropriate gut saline, respectively. The use of individual tubes for each anatomical region and piece of gut enabled collection of the serosal fluid for total Ag determination and the subsequent calculation of the apparent net transepithelial uptake of the metal. In all experiments, the serosal saline was isosmotic with that on the luminal side, but without any silver addition. The gut sacs were incubated at 15 ± 1 °C for 4 h and aerated with a 99.7% O_2 : 0.3% CO_2 gas mixture. Samples of the serosal saline were taken after 4 h from each individual tube (n = 6 per tissue/treatment). The viability of the gut sacs were assessed gravimetrically (any net flux of water should be into the gut sac in freshwater fish[21]). Any gut sac that showed appreciable weight loss (*i.e.*, loss of the contents) or a high silver concentration in the serosal saline (*i.e.*, evidence that the sutures were leaking) was discarded.

Successful gut sacs were then processed to determine the total Ag concentration by ICP-MS. For each region of the gut, the sutures were removed and the gut rinsed in 5 mL of the appropriate clean gut saline, with these luminal washings collected into a 50 mL tube for Ag determination. Tissues were then immediately dipped into a second 5 mL of gut saline containing 1 mmol L^{-1} disodium ethylenediaminetetraacetate (EDTA) as a precautionary further rinse to aid removal of any loose surface-associated material (*i.e.*, particulates and cations that were labile on the surface of the tissue). Subsequently, the tissues were blotted on 25 cm^2 squares of tissue paper (two squares for the oesophagus, mid intestine and hind intestine, four sheets for the stomach and anterior intestine). The tissue papers were stored in the tube with the EDTA saline rinse for later trace metal analysis (see below). The collection of these various washings and blotted papers enabled some ready estimate of the externally adsorbed silver, rather than the internally absorbed silver, during the experiments, although more detailed surface adsorption experiments were also performed (see below). Following the

washing and blotting, the gut mucosa was stripped from the surface of the muscularis using the edge of a microscope slide and weighed and stored at −20 °C prior to subsequent metal analysis (see below).

Tissue concentrations of Ag were routinely expressed as ng g^{-1} dry weight (dw) of tissues and net accumulation rates expressed per g dw of tissue. However, it can also be useful to express fluxes across the gut epithelium on a surface area basis. For the latter, the outline of the muscularis layer was drawn onto white paper and the surface area was calculated using ImageJ software. The fluid flux (μL cm^{-2} h^{-1}) was assessed gravimetrically according to Ojo and Wood as follows:[29]

$$\text{Fluid flux} = \frac{\Delta V}{\text{SA} \times T}$$

where ΔV (g) is the change in volume of the gut sac lumen (based on equivalent weight of water) over the 4 h exposure, SA (cm^2) is the surface area and T (h) is time.

The apparent net accumulation of metals in the gut is rarely fixed but usually varies with the exposure dose, with the fraction remaining in the gut lumen or loosely attached to the exterior of the gut mucosa also changing. It is therefore useful to express the absolute amount of total Ag measured in the washings and the different tissues as a fraction of the absolute amount of Ag in the exposure, with the latter amount being the measured concentration in ng mL^{-1} multiplied by the volume (mL × 100%). The proportions of the total Ag dose in the muscularis, mucosa and the EDTA wash were expressed as a percentage of the absolute amount of silver added to the gut lumen at the start of the incubation. The proportion of the total silver dose in the initial saline rinse to obtain the luminal washings was estimated as follows:

$$\text{Percent of Ag in luminal washing} = \frac{D_0 - (\text{Muscularis} + \text{Mucosa} + \text{EDTA})}{D_0}$$

where D_0 is the absolute amount of Ag (*i.e.* the dose, the absolute mass of total silver in ng) inserted into the gut lumen at the start of the experiment, and muscularis, mucosa and EDTA represent the mass (ng) of Ag associated with the muscularis, mucosa and the EDTA washing, respectively.

Surface binding experiment using $AgNO_3$, Ag NPs and Ag_2S NPs

To quantify the amount of Ag that was surface bound to the intestine during the gut sac experiment, a separate 'rapid solution dipping' experiment was conducted following Al-Jubory and Handy.[26] The mid and hind intestines were selected for this task because these segments of the gut could be easily everted and dipped in test solutions to quantify the adsorption of Ag to the mucosa. The tissues collected were first dipped in 500 mL of clean chloride-containing saline (described above) for 30 seconds as an initial rinse. Then the tissues were dipped in 500 mL of the same saline but containing 1 mg L^{-1} of the appropriate Ag material for 30 seconds. This duration was to mimic the instantaneous exposure of the surface of the gut sacs, but also ensuring negligible uptake into the tissues.[26] Tissues were then processed as above (*i.e.*, with a luminal wash and an EDTA rinse) prior to measurement of the total Ag concentrations (see below).

Trace metal analysis

Trace metal analysis was conducted using a similar approach to that of Shaw *et al.*[30] The total silver concentration was determined by ICP-MS in the luminal and serosal saline at the end of each experiment and in the washings from the mucosa, as well as in the tissue samples following strong acid digestion. Samples of saline collected from the experiment were acidified and diluted prior to analysis. The washings from both the initial luminal saline rinse and the subsequent EDTA rinse of the exterior surface of the mucosa (~5 mL) were acidified with 2 mL nitric acid and diluted to 20 mL with ultrapure water and then left overnight before being analysed by ICP-MS. For the EDTA wash, this enabled time for any labile silver on the surface of the blotting paper in each tube to leach into the solution. With every set of samples, procedural blanks were also performed to account for any contamination from test tubes or reagents. For the analysis of all salines and washings, the standards were matrix matched and standard curves of $AgNO_3$, Ag NPs and Ag_2S NPs in saline were compared to commercially available elemental standards. Instrument drift was monitored by the addition of internal standards (indium and iridium) and standard checks were made every 10–15 samples. The instrument limit of detection was calculated for each set of samples by multiplying the standard deviation of the lowest standard by three. The Ag detection limit for the gut saline was around 0.54 ng mL^{-1}. Measurements of the total Ag from the working stocks were 97 ± 0.14%, 98 ± 0.24% and 95 ± 5.66% of the expected nominal total Ag concentration for $AgNO_3$, Ag NP and Ag_2S NPs, respectively (mean ± S.D., n = 5).

Tissue samples of mucosa and separated muscularis were also analysed according to Shaw *et al.*[30] with minor modifications. Tissues were freeze-dried overnight (Lablyo freeze dryer), weighed and then digested in 0.2 mL of primer plus grade nitric acid for 4 h at 55 °C and diluted to 2 mL using ultrapure water. Standards were matrix matched and instrument drift checked during the sample runs as above. A certified reference tissue (Dorm 4; National Research Council Canada) was also digested as above and analysed for total Ag. Dorm 4 gave a good recovery of 112 ± 10% (mean ± S.D., n = 3). The limit of detection for Ag in the tissue digests was 0.08 ng mL^{-1}, which equates to a tissue detection limit of (mean ± S.E.M., n = 6) 40.9 ± 7.8 and 5.1 ± 0.9 ng g^{-1} dw in the mucosa and muscularis, respectively.

Dialysis experiments

Dialysis experiments were conducted with the Ag NPs or Ag_2S NPs to determine any dissolution of dissolved silver from the particles. Measurements were made in both ultrapure water and the appropriate gut saline. Two pH values were selected: pH 7.8 to simulate the gut sac exposures and pH 2 (adjusted using nitric acid to ensure the same chloride concentration) to mimic the acidity of the stomach.[31] One concern for the pH experiment was that the neutral pH would drive the binding of any Ag^+ ions to the glassware, unlike acid conditions, and thus cause artefacts in the measured silver concentration in the external solution in the beaker. To check for this phenomena, a known concentration of Ag as $AgNO_3$ (100 μg L^{-1}) was spiked directly into the gut saline at pH 2 and 7.8, and its disappearance over time was monitored. Another concern for the gut is the presence of amino acids in the lumen that might chelate any dissolved silver and so drive dissolution of the Ag NPs. Dialysis experiments were therefore also conducted in the gut saline, but in the presence of essential amino acids (0.5 mM of either L-histidine or L-cysteine). In addition, to know if the dissolution characteristics were saline-specific, a blood compartment saline (Cortland saline, in mmol L^{-1}: NaCl, 121.4; KCl, 5.1; $NaHCO_3$, 11.9; $Na_2HPO_4.H_2O$, 2.9; $CaCl_2{\cdot}2H_2O$, 1.4; and $MgSO_4{\cdot}7H_2O$, 1.9; pH 7.8) was also used to compare against the gut saline. These latter two experiments with amino acids or Cortland saline were conducted only with the Ag NPs, as Ag_2S material showed no appreciable dissolution in the earlier experiments with gut salines.

The dialysis experiments were performed similar to that of Besinis *et al.*[32] Beakers (400 mL volume) were acid washed and rinsed in ultrapure water before adding 297 mL of the respective saline. Dialysis tubing (Sigma-Aldrich, 12 000 kDa cutoff) was cut into 15 cm lengths and soaked overnight in water and then rinsed in ultrapure water. The tubing was sealed at one end with a knot and 3 mL of a 100 mg L^{-1} Ag NP stock was added to the bag. The tubing was then sealed with another knot. Once sealed, the exteriors of the dialysis bags were carefully rinsed with ultrapure water and the bags were placed in the beakers of the respective saline. The beakers were gently stirred (IKA RO 15 power magnetic stirrer) at room temperature for 4 h. For all dialysis experiments, water samples (1 mL) were taken at 0 (before dialysis bags were added to beakers), 0.25, 0.5, 1, 2 and 4 h (*i.e.*, to match the duration of the gut sac experiments). The samples were acidified immediately with 1 mL of Primar Plus trace analysis grade nitric acid. Samples were further diluted with ultrapure water to a final volume of 4 mL and analysed using ICP-MS as above using matrix matched standards.

Statistical analysis

All data were presented using mean ± S.E.M., with curve fitting and statistical analysis conducted using SigmaPlot 13.0. Data were analysed for outliers using Grubbs' test ($P < 0.05$) before checking data for normality (Shapiro–Wilk test) and equal variance (Brown–Forsythe test). Data that were normally distributed or could be $\log_{10}$ transformed to a normal distribution were analysed by either a one-way ANOVA (either for effects within saline or Ag concentrations within gut sacs from one region of the gut) or a two-way ANOVA (between treatment and tissue types and/or gut region) followed by the *post hoc* Holm–Sidak procedure. The P values presented are from Holm–Sidak tests. Where data were non-parametric and could not be transformed, either a Mann–Whitney U or the Kruskal–Wallis test was used. For dialysis experiments, the dissolution curves were fitted with a rectangular hyperbole function to the mean values.

Results

Ag exposure of gut sacs in chloride-containing medium

The nominal Ag concentrations were confirmed by ICP-MS measurement in the fresh stocks before dosing. In addition to this, the gut sac lumen contents were collected at the end of the experiment and then the tissue was rinsed in clean saline to ensure that as much as possible of the residual exposure medium was collected (the 'luminal saline' in Table 1). The Ag contents of the resulting saline from this initial rinse at the end of the experiment are shown in Table 1. The data are expressed as ng of absolute mass as the volume of the gut sac varied between anatomical regions of the gut. Nonetheless, the amounts of Ag in the rinses from the control (unexposed) gut sacs were below the detection limit, as expected (Table 1). For the $AgNO_3$ exposure, the luminal saline contained around 72–100 ng of total Ag or much higher depending on the region of the gut at the end of the experiment, confirming that the supply of Ag in the lumen remained in excess throughout. Similarly, for the Ag NP and Ag_2S NP exposures, readily detectable amounts of Ag remained in the lumen (Table 1), confirming that the exposure had persisted over the 4 h incubation.

There were also some differences in the residual Ag remaining in the gut lumen after the initial rinse according to anatomical regions of the gut (Table 1). Within the $AgNO_3$ treatment, there tended to be more Ag remaining in the lumen of the stomach and hind intestine compared to other regions of the gut, but these were not statistically different from other regions (two-way ANOVA, $F_{(4,53)} = 6.572$, $P < 0.001$, Holm–Sidak $P = 0.062$ to 0.898). Similarly for the Ag NP exposure, the highest Ag content was found in the lumen of the hind intestine (two-way ANOVA, $F_{(4,52)} = 10.068$, $P < 0.001$, Holm–Sidak $P = 0.001$), but not in the case of Ag_2S NPs where the most residual Ag was found in the lumen of the stomach ($P < 0.001$) and anterior intestine (two-way ANOVA, $F_{(4,59)} = 22.232$, $P < 0.036$).

Exposure was also confirmed by measuring the total Ag concentrations in the rinsed portions of mucosa and muscularis at the end of the experiment (Table 2). The measured Ag concentrations in tissues from control (unexposed) gut sacs remained below the detection limit. In contrast, exposure to $AgNO_3$, Ag NPs and Ag_2S NPs resulted in readily

Table 1 Confirming exposure of gut sacs to silver materials. Total mass (ng) of Ag found in the luminal saline (rinse 1) and EDTA wash (rinse 2)

Saline type	Treatment	Sample type	Oesophagus	Stomach	Anterior intestine	Mid intestine	Hind intestine
Chloride-containing	Control	Luminal saline	$<10.8^{A}$	$<10.8^{A}$	$<10.8^{A}$	$<10.8^{A}$	$<10.8^{A}$
		EDTA wash	$<10.8^{A}$	$<10.8^{A}$	$<10.8^{A}$	$<10.8^{A}$	$<10.8^{A}$
	$AgNO_3$	Luminal saline	71.9 ± 18.3^{A}	217.8 ± 56.2^{Aa}	$<10.8^{Aa}$	100.5 ± 42.7^{Aa}	311.6 ± 56.3^{Aa}
		EDTA wash	20.3 ± 7.2^{Ba}	143.7 ± 27.7^{Ac}	47.2 ± 17.5^{Aab}	76.4 ± 10.1^{Abc}	67.4 ± 22.4^{Babc}
	Ag NPs	Luminal saline	53.4 ± 25.0^{Aab}	100.8 ± 28.5^{Ab}	26.11 ± 15.4^{Aa}	90.8 ± 16.7^{Ab}	378.8 ± 69.6^{Ac}
		EDTA wash	36.9 ± 7.3^{A}	66.2 ± 9.0^{Aa}	45.6 ± 10.6^{Ba}	42.97 ± 9.4^{Aa}	49.8 ± 10.8^{Ba}
	Ag_2S NPs	Luminal saline	13.2 ± 3.9^{Aabc}	378.3 ± 80.4^{Aab}	217.9 ± 77.5^{Ac}	52.4 ± 10.3^{Aab}	14.7 ± 4.9^{Ac}
		EDTA wash	16.1 ± 3.1^{Ab}	69.2 ± 14.5^{Ba}	6.3 ± 1.6^{Ba}	28.1 ± 6.1^{Ac}	5.3 ± 1.7^{Ab}
Chloride-free	Control	Luminal saline	<10.8	<10.8	<10.8	<10.8	<10.8
		EDTA wash	<10.8	<10.8	<10.8	<10.8	<10.8
	$AgNO_3$	Luminal saline	<10.8	202.8 ± 56.2^{Aa}	<10.8	85.6 ± 42.6^{Aa}	296.6 ± 56.3^{Aa}
		EDTA wash	<10.8	127.6 ± 27.7^{Aa}	52.1 ± 17.9	63.2 ± 10.1^{Aa}	61.6 ± 24.3^{Aa}
	Ag NPs	Luminal saline	<10.8	85.9 ± 28.5^{Aab}	<10.8	44.36 ± 22.6^{Aa}	363.9 ± 69.6^{Ab}
		EDTA wash	<10.8	74.6 ± 41.2^{Aa}	36.4 ± 5.7	20.8 ± 11.0^{Aa}	29.8 ± 12.0^{Aa}

Data are mean ± S.E.M (n = 5/6). Different upper case letters denote significance between rinse 1 and 2. Different lower case letters denote statistical differences between gut regions (rows; two-way ANOVA). No difference between gut regions of the chloride-free $AgNO_3$ and Ag NP treatments (two-way ANOVA). No significant difference between the gut regions of the chloride-free $AgNO_3$ treatment (two-way ANOVA). The limit of detection of the instrument was 0.54 ng mL^{-1} which equates to 10.8 ng Ag in the luminal and EDTA washes.

detectable total Ag in both the mucosa and the muscularis in all regions of the gut (Table 2).

Unsurprisingly, the gut mucosa, being the uppermost external facing tissue, showed much higher concentrations of total Ag than the equivalent underlying muscularis regardless of the type of Ag exposure (Table 2). In most cases, two thirds or more of the accumulated Ag was associated with the mucosa rather than the muscularis. Two-way ANOVA revealed both gut region ($F_{(4,85)}$ = 3.071, P = 0.022) and treatment ($F_{(2,85)}$ = 5.281, P = 0.007) related differences in the mucosa. For the $AgNO_3$ exposure, there was a tendency for more Ag to accumulate in the mucosa of the mid intestine, although this was not statistically significant from the other regions in the gut (P = 0.458 to 0.998). Similar observations were made for the mucosa from gut sacs exposed to Ag NPs or Ag_2S NPs. However, for the Ag_2S NP treatment, the total Ag concentration in the mid intestine was significantly higher than that in the anterior intestine (P = 0.022). Within treatment, the Ag associated with the mucosa of the mid intestine of Ag_2S NP (P = 0.043) treatment was significantly elevated compared to the mid intestine of the Ag NP treatment; indicating a material-type effect within the mid intestine.

The two-way ANOVA of the concentration of total Ag in the muscularis (Table 2) showed statistically significant differences overall for both the gut region ($F_{(4,83)}$ = 12.988, $P < 0.001$) and type of treatment ($F_{(2,83)}$ = 105.292, $P < 0.001$). In most cases, there was statistically more Ag in the muscularis from the $AgNO_3$ exposure than either of the nano forms, indicating that the nano forms were less bioavailable to this tissue. However, there were also some small but statistically

Table 2 The concentration of Ag in the tissues (ng g^{-1} dw) and the percentage of Ag in the mucosa following 4 h of exposure

Saline type	Treatment	Sample	Oesophagus	Stomach	Anterior intestine	Mid intestine	Hind intestine
Chloride-containing	$AgNO_3$	Mucosa	1303.6 ± 398.7^{Aa}	1165.6 ± 295.4^{Aa}	1301.7 ± 445.1^{Aa}	3961.7 ± 1254.5^{ABa}	1508.9 ± 375.3^{Aa}
		Muscularis	72.4 ± 27.5^{Aa}	76.4 ± 16.3^{Aa}	289.1 ± 36.1^{Ab}	457.2 ± 110.9^{Ab}	518.2 ± 66.9^{Ab}
		% in mucosa	58.0 ± 9.0^{Aa}	63.7 ± 7.6^{Aa}	63.7 ± 5.5^{Aa}	74.8 ± 4.4^{Aa}	59.3 ± 4.0^{Aa}
	Ag NPs	Mucosa	747.6 ± 317.5^{Aab}	395 ± 68.7^{Aab}	610.0 ± 155.7^{Aa}	1506.9 ± 907.5^{Bb}	732.3 ± 258.7^{Aab}
		Muscularis	32.4 ± 6.5^{ABa}	39.0 ± 5.8^{Aa}	45.3 ± 8.3^{Ba}	38.0 ± 8.2^{Ba}	57.0 ± 6.6^{Ba}
		% in mucosa	71.4 ± 5.2^{Aab}	59.5 ± 3.7^{Aa}	90.2 ± 1.7^{Bc}	84.6 ± 3.8^{Bbc}	84.4 ± 4.3^{Bbc}
	Ag_2S NPs	Mucosa	852.6 ± 330.1^{Aa}	595.0 ± 106.1^{Aa}	327.9 ± 78.1^{Aa}	5145.5 ± 1944.4^{Aa}	2610.7 ± 628.0^{Aa}
		Muscularis	13.5 ± 1.6^{Ba}	13.1 ± 2.0^{Ba}	26.7 ± 8.6^{Bba}	38.5 ± 19.5^{Bab}	42.9 ± 10.3^{Bb}
		% in mucosa	77.6 ± 5.8^{Aa}	90.2 ± 1.3^{Bab}	90.6 ± 2.1^{Bb}	98.5 ± 0.6^{Cc}	96.8 ± 0.4^{Cd}
Chloride-free	$AgNO_3$	Mucosa	954.0 ± 439.4^{Aa}	1777.8 ± 680.0^{Aa}	527.7 ± 164.0^{Aa}	3278.0 ± 1156.2^{Aa}	1629.3 ± 477.5^{Aa}
		Muscularis	86.6 ± 23.8^{Aa}	65.6 ± 8.2^{Aa}	$144.1 \pm 23.3^{Aab*}$	488.3 ± 165.8^{Ab}	641.0 ± 110.8^{Ab}
		% in mucosa	49.1 ± 9.2^{Aa}	74.4 ± 5.3^{Ab}	60.9 ± 9.4^{Ab}	82.5 ± 11.1^{Ab}	41.9 ± 8.6^{Aa}
	Ag NPs	Mucosa	416.5 ± 245.8^{Bab}	462.8 ± 182.3^{Bab}	$95.6 \pm 16.7^{Aa*}$	2729.5 ± 1016.8^{Ab}	1976.1 ± 1110.7^{Ab}
		Muscularis	19.0 ± 4.8^{Ba}	30.5 ± 9.3^{Bb}	31.1 ± 5.4^{Bb}	$88.6 \pm 21.9^{Bbc*}$	273.0 ± 117.9^{Bc}
		% in mucosa	51.8 ± 3.1^{Aa}	69.2 ± 13.5^{Aab}	72.3 ± 4.5^{Aab}	93.3 ± 1.5^{Ab}	56.6 ± 7.7^{Ba}

Data are mean ± S.E.M (n = 5/6). % in mucosa = mass in mucosa/mass in mucosa + mass in muscularis × 100. Unexposed controls are not shown due to being below the LOD of the ICP-MS. Different lower case letters denote statistical differences between regions of the gut (rows). Different upper case letters denote statistical differences between treatment within the same sample type (but within saline type; columns). (*) denotes significant difference between same tissue but exposed to chloride-containing saline. No letters or * means no significant difference between tissues or treatments.

significant differences between the total Ag accumulated in the muscularis from exposure to Ag NPs compared to the Ag_2S NPs, with generally less Ag accumulated from exposure to Ag_2S NPs (Table 2). The anatomical region of the gut was also important and within the muscularis of the $AgNO_3$ treatment, the anterior, mid and hind intestine showed significantly elevated total Ag concentrations compared to both the oesophagus and the stomach (all values $P < 0.001$). A similar pattern was observed for the gut region effect in the Ag_2S treatment, where the stomach was significantly higher compared to the oesophagus ($P = 0.024$) and stomach ($P = 0.049$). However, there was no significant difference between gut regions within the Ag NP treatments for the muscularis ($P > 0.05$).

Ag exposure of gut sacs in chloride-free medium

The results of the experiments using a nominally chloride-free saline were almost identical to those with the chloride-containing saline, indicating that the exposure (Table 1) and Ag accumulation in the tissue (Table 2) were largely unaffected by the removal of chloride. In the washing from the chloride-free experiment, as expected the Ag concentrations from the unexposed controls remained below the detection limit. However, silver from both $AgNO_3$ and Ag NP exposures was detected in the luminal and EDTA washes at the end of the exposure, confirming that the metal was in excess in the lumen throughout the experiments (Table 1). Both the $AgNO_3$ and the Ag NP treatments had a tendency for more Ag to be found in the washings from the stomach and hind intestine compared to the other regions of the gastrointestinal tract; yet a two-way ANOVA ($F_{(4,37)} = 4.850$, $P = 0.004$) revealed that only the washings from the Ag NP exposure to the hind intestine had a significantly higher amount of Ag compared to that remaining following exposure of the mid intestine ($P = 0.027$). There was no significant difference between the amount of total Ag recovered in the EDTA wash in either treatment with respect to anatomical regions of the gut.

The gut tissue itself also showed elevated total Ag concentrations following exposure to $AgNO_3$ or Ag NPs in chloride-free saline (Table 2), while the unexposed controls remained below the detection limit. Some anatomical regions of the gut also showed more total Ag accumulation from exposure to $AgNO_3$ compared to Ag NP, indicating that the metal salt was more bioavailable than the nanomaterial. Similar to the findings with chloride-containing saline, typically around two thirds of the Ag was associated with the mucosa rather than the underlying muscularis in chloride-free conditions, regardless of the form of Ag presented (Table 2). For the mucosa tissue, two-way ANOVAs revealed some overall gut anatomical region ($F_{(4,54)} = 7.518$, $P < 0.001$) and treatment ($F_{(1,54)} = 6.885$, $P = 0.012$) effects. However, the $AgNO_3$ treatment showed no significant difference of total Ag concentration in the mucosa with anatomical region of the gut. In contrast, the mucosa from the Ag NP treatment had significantly more total Ag in the mid ($P < 0.001$) and hind ($P = 0.004$) intestine compared to the anterior intestine. Additionally for the mucosa, some small but statistically significant differences were observed between the treatments in chloride-free saline with anatomical region of the gut. For example, the stomach of the $AgNO_3$ treatment had significantly more Ag compared to that of the Ag NP treatment ($P = 0.037$).

The muscularis of gut sacs exposed to either $AgNO_3$ or Ag NPs also showed readily measurable total Ag concentrations, albeit less than the equivalent mucosa. A two-way ANOVA showed that the concentration of total Ag within the muscularis was dependent on the gut region ($F_{(4,55)} = 21.686$, $P < 0.001$) and treatment ($F_{(1,55)} = 56.802$, $P < 0.001$; Table 2) in chloride-free conditions. For example, the mid ($P = 0.001$) and hind intestine ($P < 0.001$, respectively) of the $AgNO_3$ treatment has significantly higher Ag concentrations compared to the oesophagus or the stomach ($P < 0.001$). Similar observations were made for the anatomical region of the gut within the Ag NP exposures, with the muscularis of the mid ($P < 0.001$) and hind ($P = 0.001$) intestine having significantly higher Ag concentrations compared to the oesophagus.

Despite some treatment effects within the experiment with chloride-free saline, overall the replacement of chloride with other anions had absolutely no effect on the total amount of Ag recovered in the gut washings (Table 1). The removal of chloride from the saline did not increase Ag accumulation in the tissues and mostly had no effects, except for a decrease in total Ag in the muscularis of the anterior intestine of the $AgNO_3$ treatment in chloride-free conditions (one-way ANOVA, $F_{(1,11)} = 11.396$, $P = 0.007$). Within the muscularis of the mid intestine for Ag NP treatment, there was significantly more total Ag in tissue from the chloride-free saline compared to the chloride-containing saline (one-way ANOVA, $F_{(1,10)} = 5.416$, $P = 0.045$).

Surface bound Ag and partitioning of total Ag in the gut tissue

The luminal saline rinses and EDTA washes of the gut sac tissue at the end of the main experiments (Table 1) were useful to demonstrate that the total Ag remained in excess in the gut lumen (*i.e.*, the luminal contents could not be rate limiting for apparent uptake). The EDTA wash attempted to remove any labile fraction from the surface of the mucosa. This fraction (unsurprisingly) often had less total Ag than the initial rinse in luminal saline, but it did show that a surface-associated EDTA-extractable fraction was present. A separate surface binding experiment was therefore conducted to investigate the phenomena in more detail under conditions were chloride was present (Fig. 2).

The latter experiment used the mid and hind intestine because those regions of the gut had shown the most Ag accumulation (Table 2). Fig. 2 shows the Ag remaining on the surface of the tissue after a 30 second exposure and rinses to remove any labile or EDTA extractable fraction. The exposure time was too short for true internal uptake of Ag (regardless of form) and the Ag measured represents that which is

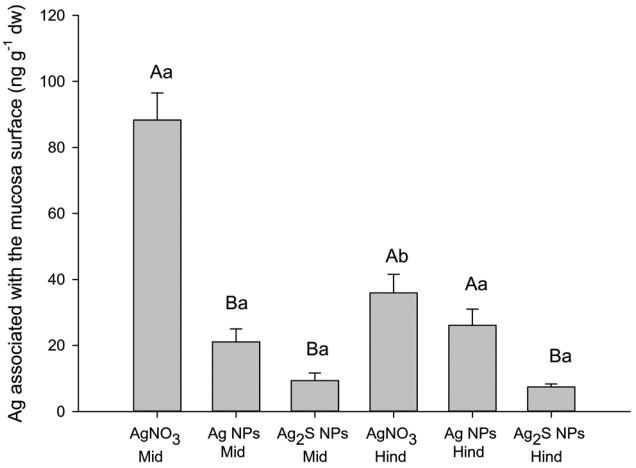

Fig. 2 The concentration of total Ag associated with the surface of the mid and hind intestine following the surface binding experiment. Data are mean ± S.E.M (n = 5). Upper case letters denote statistical differences within the same tissue type. Different lower case letters denote statistical differences between gut regions within the same treatment.

associated with the surface of the mucosa but not easily removed by washing. The concentrations of Ag measured were low, <90 ng g^{-1} dw or much less (Fig. 2). There were some material-type effects on the apparent surface binding (Fig. 2) with more surface-bound Ag from $AgNO_3$ (unsurprising for dissolved silver) compared to the nano forms; and with Ag_2S binding the least. For example, a two-way ANOVA ($F_{(2,27)}$ = 53.064, $P < 0.001$) revealed that the surface-associated Ag from the $AgNO_3$ exposure to the mid intestine was significantly greater than that for both the Ag NP ($P < 0.001$) and Ag_2S NP ($P < 0.001$) treatments. The surface-associated Ag from the $AgNO_3$ exposure to the hind intestine was significantly elevated compared to that of the Ag_2S treatment (two-way ANOVA $F_{(1,27)}$ = 13.888, $P < 0.001$).

Regardless of any treatment effects on surface binding, the values (Fig. 2) are in contrast to the hundreds of ng g^{-1} dw measured in the tissues from the main experiments (Table 2). This indicates that only a small fraction (<5%) of the total Ag measured in the gut sacs from the main experiments (Table 2) is surface associated and that most of the Ag (form unknown) was inside the mucosa. The apparent net Ag accumulation rates into the mucosa are shown in Table 3 for the main experiments. The values reflect the original measured concentrations of Ag in the gut tissue (Table 2), with apparent net Ag uptake rates of a few nmol g^{-1} h^{-1} (Table 3). The apparent Ag accumulation rates were not attributed to passive water movement (*i.e.*, solvent drag) as the water fluxes were small and sometimes in the opposite direction to the Ag flux (Table 3).

The partitioning of the exposure dose of Ag is shown in Table 4. The majority of the dose on a percentage basis remained in the lumen, or was removed by the EDTA wash, leaving only a few percent of the original dose in the mucosa and even less in the muscularis (Table 4). This demonstrates that the bioavailability of Ag is only a few percent of the exposure dose regardless of the form of Ag used and with the mid and hind intestine being more important than other regions of the gastrointestinal tract (Table 4). There is perhaps one exception, where the mucosa of the mid intestine was calculated to contain 19.7% of the Ag from Ag_2S (Table 4). Also, the anterior intestine contains the pyloric caeca, where between 30–54% of the total dose was localised. One-way ANOVA revealed no significant difference between the concentration of Ag associated with the caeca by treatment

Table 3 Fluid flux and rate of accumulation into the mucosa of all materials in either chloride-containing or chloride-free saline

		Oesophagus	Stomach	Anterior intestine	Mid intestine	Hind intestine
Fluid flux (mL g^{-1} h^{-1})						
Chloride-containing	Control	0.05 ± 0.12^{a}	−0.04 ± 0.01^{a*}	1.61 ± 1.49^{a}	0.03 ± 0.18^{a}	−0.12 ± 0.06^{a}
	$AgNO_3$	0.19 ± 0.24^{a}	−0.02 ± 0.02^{a}	0.81 ± 0.57^{a}	0.22 ± 0.13^{a}	−0.11 ± 0.04^{a}
	Ag NPs	0.13 ± 0.06^{a}	0.16 ± 0.09^{a}	2.79 ± 1.23^{a}	0.03 ± 0.28^{a*}	0.12 ± 0.36^{a}
	Ag_2S NPs	−0.03 ± 0.10^{a}	−0.06 ± 0.04^{a}	0.27 ± 0.58^{a}	0.91 ± 0.41^{a}	0.59 ± 0.45^{a}
Chloride-free	Control	−0.07 ± 0.07^{a}	0.03 ± 0.02^{a}	0.03 ± 0.06^{a}	−0.19 ± 0.08^{a}	−0.16 ± 0.19^{a}
	$AgNO_3$	0.11 ± 0.07^{a}	0.05 ± 0.02^{a}	0.12 ± 0.24^{a}	−0.19 ± 0.09^{a}	−0.10 ± 0.25^{a}
	Ag NPs	−0.03 ± 0.08^{a}	0.05 ± 0.02^{a}	0.28 ± 0.20^{a}	−0.17 ± 0.09^{a}	−0.17 ± 0.14^{a}
Accumulation rate into mucosa (nmol g^{-1} h^{-1})						
Chloride-containing	Control	ND	ND	ND	ND	ND
	$AgNO_3$	2.31 ± 0.75^{Aa}	2.72 ± 0.69^{Aa}	3.04 ± 1.04^{Aa}	9.26 ± 2.93 ^{ABa}	3.53 ± 0.88^{Aa}
	Ag NPs	4.08 ± 2.40^{Aa}	0.92 ± 0.16^{Aa}	1.43 ± 0.36^{Aa*}	3.52 ± 2.12^{Ba}	1.71 ± 0.60^{Aa}
	Ag_2S NPs	1.99 ± 0.77^{Aab}	1.39 ± 0.25^{Aab}	0.77 ± 0.18^{Aa}	12.02 ± 4.07^{Ab}	6.10 ± 1.47^{Aab}
Chloride-free	Control	ND	ND	ND	ND	ND
	$AgNO_3$	2.23 ± 0.93^{Aa}	4.15 ± 1.59^{Aa}	1.23 ± 0.38^{Aa}	7.66 ± 2.70^{Aa}	3.73 ± 1.12^{Aa}
	Ag NPs	0.97 ± 0.57^{Bab}	1.08 ± 0.43^{Bab}	0.20 ± 0.03^{Aa}	7.48 ± 2.57^{Ab}	5.36 ± 3.05^{Ab}

Data are mean ± S.E.M (n = 5/6). ND indicates an accumulation rate cannot be determined due to tissue concentration being below the LOD of the ICP-MS. No significant difference in the fluid fluxes between treatments. Lower case letters denote statistical differences between gut regions in the same treatment (rows). Upper case letters denote statistical differences between treatments (columns). (*) denotes significant effect between saline (Kruskal–Wallis).

Table 4 Partitioning of Ag distribution throughout the gut sac. The rinse 1, rinse 2, the mucosa and muscularis expressed as the percentage of Ag dosed at the start of the 4 h incubation

Treatment	Region of gut	Luminal rinse	EDTA wash	Caeca	Mucosa	Muscularis
$AgNO_3$	Oesophagus	80.5 ± 5.4^{a}	$13.7 \pm 6.0^{ab*}$	—	$3.8 \pm 1.9^{*}$	$2.1 \pm 0.7^{*}$
	Stomach	76.6 ± 4.2^{a}	$17.7 \pm 3.6^{Aa*}$	—	$3.8 \pm 1.1^{*\#}$	$1.8 \pm 0.4^{*\#}$
	Anterior	41.5 ± 2.4^{Ab}	4.5 ± 1.5^{Ab}	$48.1 \pm 3.3^{\#\wedge>}$	3.7 ± 0.7	$2.2 \pm 0.6^{A*}$
	Mid	65.8 ± 3.3^{a}	22.4 ± 2.5^{Aa}	—	$8.9 \pm 1.9^{A*\#}$	$2.9 \pm 0.7^{A*\#}$
	Hind	82.1 ± 3.4^{a}	$9.4 \pm 2.3^{Aab*}$	—	$5.3 \pm 1.2^{*}$	$3.2 \pm 0.5^{A*}$
Ag NPs	Oesophagus	69.9 ± 9.3^{a}	$23.1 \pm 6.0^{a*}$	—	$1.8 \pm 0.5^{*\#}$	$1.2 \pm 0.4^{ab*\#}$
	Stomach	81.8 ± 5.1^{a}	14.8 ± 5.1^{ABab}	—	$2.1 \pm 0.7^{*}$	$1.4 \pm 0.4^{a*}$
	Anterior	39.4 ± 8.1^{Ab}	4.1 ± 0.8^{Ab}	$54.0 \pm 7.9^{\#\wedge>}$	2.1 ± 0.6	$0.4 \pm 0.2^{Bb*\wedge}$
	Mid	78.0 ± 4.9^{a}	18.2 ± 3.8^{Ab}	—	3.5 ± 1.9^{B}	$0.3 \pm 0.1^{Bb*}$
	Hind	88.8 ± 1.9^{a}	$7.6 \pm 2.1^{Aab*}$	—	$3.1 \pm 1.1^{*\#}$	$0.5 \pm 0.2^{Bab*\wedge}$
Ag_2S NPs	Oesophagus	78.1 ± 3.8^{ab}	$12.3 \pm 1.7^{a*}$	—	$7.8 \pm 2.5^{ab*}$	$1.8 \pm 0.6^{a*\#}$
	Stomach	87.6 ± 1.7^{ab}	5.6 ± 1.2^{Bab}	—	6.1 ± 0.8^{ab}	$0.7 \pm 0.1^{ab*}$
	Anterior	67.0 ± 8.0^{Ba}	0.3 ± 0.1^{Bc}	$30.3 \pm 7.4^{\#\wedge>}$	$2.0 \pm 0.6^{a*}$	$0.2 \pm 0.1^{Bc*\wedge}$
	Mid	75.6 ± 6.3^{ab}	4.5 ± 1.2^{Bb}	—	19.7 ± 6.3^{Ab}	$0.2 \pm 0.1^{Bc*}$
	Hind	$90.9 \pm 2.6^{b\#}$	0.5 ± 0.1^{Bc}	—	8.3 ± 2.7^{ab}	$0.2 \pm 0.0^{Bbc*\wedge}$

Data are mean ± S.E.M (n = 5/6). Upper case letters denote differences between treatments within the same gut region (columns). Lower case letters denote differences between gut regions in the same fraction and treatment (columns). For significant differences between fractions within rows, (*) denotes different to rinse 1, (#) denotes different to rinse 2, (^) denotes different to mucosa and (>) denotes different to muscle. There was no Ag detected in the serosal saline (transepithelial uptake). —, not applicable to this anatomical region of the gut.

($F_{(2,16)}$ = 3.445, P = 0.061). The pyloric caeca are blind-ending tubes and these values for the caeca likely contain some Ag that was impossible to rinse out of the tissue, reflecting the lower fractions of Ag also recovered from the luminal rinse of the anterior intestine (Table 4).

Dialysis experiments in pure water and physiological salines

These experiments were conducted to explore the possibility of dissolved silver release from the Ag NPs and Ag_2S NPs. For the Ag_2S NPs no silver could be detected in the external compartment of the beakers, for either pure water or salines at pH 7.8 or pH 2. The instrument detection limit for Ag_2S was 0.2 μg L^{-1} as silver. However, dissolution curves could be constructed for the Ag NPs (Fig. 3), but the dissolution was only a few μg L^{-1} of dissolved silver (<1% of the silver added) in most cases. For example, in ultrapure water at pH 7.8 there was a steady time-dependent rise in Ag concentration in the beaker over 4 h that fitted a rectangular hyperbola (Fig. 3A), reaching a silver concentration of 1.8 ± 1.5 μg L^{-1} by the end of the experiment. This represents dissolution of 0.18% of the total Ag present in the dialysis bag, and the maximum rate of dissolution during the first few minutes of the experiment was 0.03 μg min^{-1}. There was a similar response for ultrapure water at pH 2 (Fig. 3B), although the curve reached a plateau within the first hour (0.9 ± 0.5 μg L^{-1}), representing 0.09% dissolution of the Ag NPs and with a maximum dissolution rate of 0.53 μg min^{-1}.

At pH 7.8, the concentration of dissolved Ag released into the normal gut saline (containing chloride) over 4 h was 6.2 ± 0.8 μg L^{-1} (Fig. 3C) and not statistically different to that in ultrapure water at neutral pH (P = 0.093). The dissolution in the gut saline was 0.87% of the Ag added to the dialysis bag, with a maximum dissolution rate of 0.03 μg min^{-1} at pH 7.8. However, the dissolution was greater in the gut saline under acid conditions (pH 2, Fig. 3D). A one-way ANOVA ($F_{(6,20)}$ = 10.117, P < 0.001) revealed some significant differences between the final concentration of Ag released from Ag NPs in medium after 4 h, and for gut saline at pH 2 this was significantly higher (21.3 ± 10.0 μg L^{-1}) compared to that of ultrapure water at the same pH (P = 0.002). However, even this greater Ag release represented only 2.13% and with a maximum dissolution rate of 0.09 μg min^{-1} at pH 2 in gut saline. These differences in pH effects could not be attributed to artefacts such as the pH-dependent binding of dissolved Ag to the glassware because time course controls spiked with $AgNO_3$ directly into the beakers showed 104% recovery at both pH 7.8 and 2.

The presence of amino acids in the gut saline did not enhance silver dissolution. Additions of histidine (Fig. 3E) had no effect on the release of dissolved silver compared to the gut saline without histidine (P = 0.058); resulting in 1.3 ± 0.4 μg L^{-1} of dissolved Ag in the beakers at the end of the experiment. This was 0.13% of the initial Ag present, with a maximum dissolution rate of 0.23 μg min^{-1} in the presence of histidine. In contrast, the presence of cysteine caused a significant reduction in the concentration of Ag released compared to the same saline without amino acids (P = 0.010). The cysteine containing saline had a silver concentration of 0.9 ± 0.6 μg L^{-1} by the end of the experiment (Fig. 3F), representing 0.09% dissolution and a maximum rate of dissolution of 0.12 μg min^{-1}.

Cortland saline was also tested (Fig. 3G) as a fluid that represents the serosal compartment (*i.e.*, the blood). There was 2.1 ± 1.0 μg L^{-1} release of Ag from Ag NPs after 4 h (not statistically different from the gut saline, P = 0.863); representing 0.45% dissolution and with a maximum rate of 0.45 μg min^{-1}.

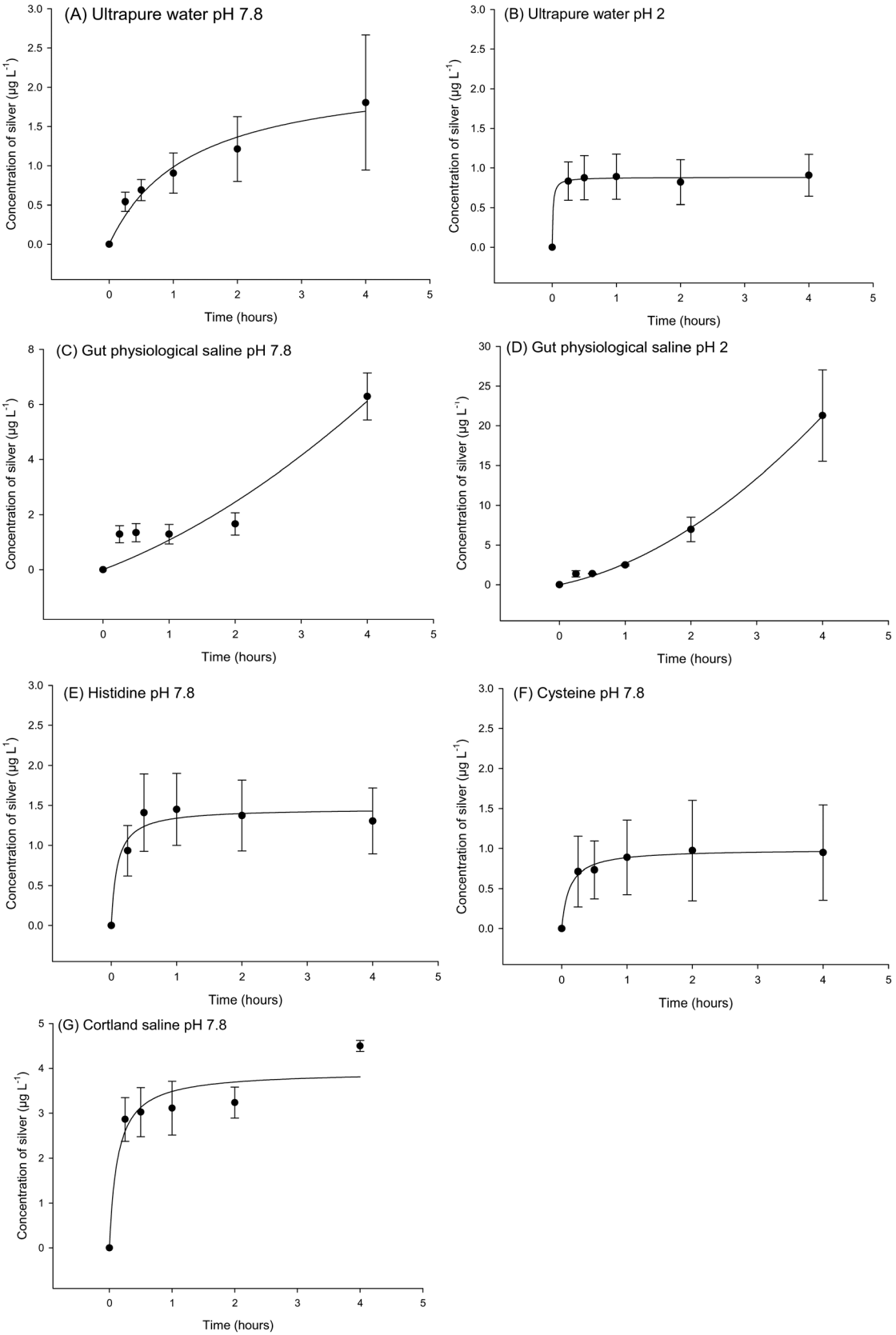

Fig. 3 Dialysis curves for the release of total dissolved silver from Ag NPs in ultrapure water at pH 7.8 (A) and 2 (B), gut physiological saline at pH 7 (C) and 2 (D), gut physiological saline + histidine (E), gut physiological saline + cysteine (F), and Cortland's saline (G). Data are mean ± S.E.M (n = 3). Curves were fitted with the equation $y = a \times x/(b + x)$. The values for a, b and r^2 were (A) 2.23, 1.27 and 0.96, (B) 0.88, 0.01 and 0.99, (C) −8.25, −9.3 and 0.90, (D) −19.22, −7.61 and 0.99, (E) 1.46, 0.09 and 0.95, (F) 0.99, 0.12 and 0.99, and (G) 3.93, 0.12 and 0.92, respectively.

Discussion

This study has demonstrated the utility of the gut sac method and found that the mid and hind intestines are especially important to total Ag accumulation in the gut regardless of the form of silver added. In most cases, the metal salt showed slightly more total Ag accumulation than either ENM. However, regardless of material added, the bioavailability was mostly only a few percent of the exposure dose, as expected for the gut as a biological barrier. Dialysis experiments showed very low or negligible dissolution of Ag NPs and Ag_2S NPs in the gut physiological saline used, indicating that the NPs remained in the particulate form in the gut lumen.

Bioavailability of the metal salt and nanomaterials in the gut lumen

The first step in dissolved metal or ENM uptake is the presentation of the test substance in the gut lumen. For $AgNO_3$ at neutral pH in the presence of millimolar concentrations of chloride found in the saline, a sparingly soluble AgCl complex is spontaneously formed (AgCl particles about 25 nm, see ref. 32). The presence of AgCl was also predicted from chemical speciation calculations with Visual MINTEQ. Consequently, much of the silver would precipitate onto the mucus covering the gut surface and be readily washed off (as observed, Table 1). Thus, the bioavailability of Ag from $AgNO_3$ exposure was very modest (<9% of the exposure dose, Table 4).

In the case of the ENMs, a similar situation may apply. Reasonable dispersions were formed in ultrapure water, but the high ionic strength of the gut saline caused some particle settling (Fig. 1). Nonetheless, the freshly made gut saline used for dosing contained particles (Fig. 1). The particle size distribution in gut saline was also measured after 4 hours (no tissue present), but the particle number concentrations were too low to obtain reliable tracks by NTA. This showed that both types of silver NPs would settle quickly from the gut saline and therefore be delivered to the surface of the tissue (measured as total Ag, Table 1), as previously observed with TiO_2 NPs.[26]

One concern for the gut lumen is whether the ENMs remain as particles or simply dissolve in the gut saline. Silver sulphide particles are regarded as persistent in environmental matrices.[4] This was the case in the gut lumen over 4 h. In the dialysis experiments, there was no detectable dissolved Ag released from the Ag_2S NPs, not even at the acidic pH 2 representative of the stomach. The Ag NPs showed some dissolution, but it was only a few $\mu g\ L^{-1}$ of dissolved Ag, and represented <1% of the total silver present at neutral pH (Fig. 3). This is consistent with our previous findings for Ag NPs in salines.[32] Increasing the acidity to pH 2 caused only small further increases in dissolved Ag (Fig. 3, <3% of the silver), indicating that the Ag NPs remained as particles. In any event, the $\mu g\ L^{-1}$ amounts of dissolved Ag released would be partly complexed with the excess chloride (as above) or bind to the mucus layer (see review on fish mucus[33]). Mucus was observed, as expected, in the gut sacs during the experiments.

Silver ions also bind avidly to the –SH groups on proteins and free amino acids,[34] and one concern is that any residual amino acids in the gut sacs might drive silver dissolution from the Ag NPs. There were no amino acids in the gut saline used for the exposures, and the gut sacs were carefully washed and from unfed fish, so the problem is unlikely. The dialysis experiments also showed no effect of histidine on particle dissolution, but the presence of cysteine caused dissolution to decrease, contrary to expectations.[35] It is possible that the saline conditions used here could mask the effects of the cysteine, although the mechanism is unclear. Alternatively, cysteine might covalently bond to the surface of the particles to form a stable layer that reduces further dissolution.[36] Regardless of the details of the gut lumen chemistry, together the observations from all the dialysis experiments (Fig. 3) and the particle aggregation in gut saline (Fig. 1) indicate that particles would have been presented to the gut lumen. However, the bioavailability was low with most of the total Ag being removed in the luminal and EDTA washings (Table 1) and only a few percent of the dose remaining in the mucosa (Table 4).

Total silver accumulation in the gut tissue

This study attempted to show total Ag accumulation in the tissue (form unknown inside the cells) under physiological conditions, and to differentiate the apparent accumulation in the gut tissue from any surface-associated fraction. The gut sacs were viable and showed normal water fluxes (Table 3) and moisture content (Table S1†); comparable to our previous reports with trout gut.[26] The luminal and EDTA washing procedure attempted to remove most of the surface-associated fraction (Table 1), but with the convoluted topography of the gut, the presence of mucus, and the polyanionic nature of the epithelial surface, some external total Ag inevitably would remain. This was quantified in the rapid solution dipping experiment (Fig. 2) and shows around 90 $ng\ g^{-1}$ dw or less of surface-associated total Ag on the mid and hind intestine. For $AgNO_3$ exposure to the mucosa of the mid intestine this equates maximally to ~2% of the apparent accumulation in the tissue (3961 $ng\ g^{-1}$ dw, Table 2). For Ag NPs the 20 $ng\ g^{-1}$ dw of surface-associated Ag equates to <2% of the apparent accumulation in the tissue (1506 $ng\ g^{-1}$ dw, Table 2), similarly for Ag_2S NPs in the mucosa of the mid intestine (<1%). It is therefore possible to interpret the measured total Ag concentrations in the tissue (Table 2) as mainly accumulation into, not on, the mucosa.

The apparent accumulation for $AgNO_3$ would involve the diffusion of any dissolved silver present into the epithelial cells from the gut lumen and with the electrochemical gradient. It is likely to be physiological uptake through a carrier-mediated pathway because the water flux was in the opposite direction to the highest rates of Ag accumulation (Table 3). Solvent drag with incidental passive uptake of soluble metal

is therefore excluded. It was also hoped to demonstrate a dissolved silver involvement in uptake by removing the chloride from the physiological saline. This would, in theory, do two things: (i) increase the dissolved Ag^+ fraction in the gut lumen as AgCl formation would be less likely, and (ii) demonstrate the competitive NaCl-dependent nature of silver uptake (through apical Na^+ channels[37]). However, the removal of chloride failed to show any appreciable effects on either the amounts of total Ag recovered in the luminal and EDTA washing (Table 1) or on the Ag accumulation in the tissue (Table 2). With the benefit of hindsight, this manipulation failed because the intact epithelium is secretory and a few millimoles of chloride ion activity will always be present in the mucus layer.[38] Any Ag^+ would therefore be rapidly converted to AgCl in the microenvironment at the gut surface. The facilitated diffusive uptake of Ag^+ through epithelial ion channels is also dependent on the overall inward electrochemical gradient; but the transepithelial potential across the gut remains unchanged with symmetrical removal of chloride from both the luminal and the serosal solutions.[21] Interestingly, without the complexity of the real tissue, trout gut epithelial cell cultures do show the expected chloride dependence.[20] This highlights the importance of cell cultures for illuminating details of uptake mechanisms in individual cell types, while the gut sac approach can show the integrated effect at tissue and organ level.

Nevertheless, the accumulation rates in the gut for total Ag from $AgNO_3$ exposure were around a few nmol g^{-1} h^{-1}, with some of the highest rates in the mid intestine (Table 3). Considering the gut sac is a closed system where concentrations will come into equilibrium more quickly, these values are not inconsistent with previous reports on the net uptake rates of metals into the blood across perfused intestines (Cu, 1 μmol g^{-1} h^{-1} or less,[21] Hg, 1–2 μmol g^{-1} h^{-1} (ref. 23)). The accumulation rates for gut from the present study were also calculated on the basis of tissue surface area (see the ESI,† Table S1). Ojo and Wood[29] report tissue accumulation rates of around 250–100 pmol cm^{-2} h^{-1} in the mid and hind intestine for additions of 5.3 mg L^{-1} of dissolved Ag over 4 h. Considering that the dose was more than five times that used here, the values of around 20 pmol cm^{-2} h^{-1} for the mid and hind intestine with $AgNO_3$ (Table S1†) are not that dissimilar.

There are few reports of ENM accumulation rates in the gut tissue of fish. Al-Jubory and Handy[26] reported an accumulation of around 0.02 μmol g^{-1} of Ti for TiO_2 NPs over 4 hours in the mid and hind intestine of trout, equivalent to a total Ti accumulation rate into the mucosa of about 5 nmols g^{-1} h^{-1}, and in keeping with the accumulation rates for Ag in the mucosa here (Table 3). Interestingly, the values (Table 3) are also consistent with the maximum influx rates for the estuarine snail, *Peringia ulvae*, exposed to Ag NPs of around 90 nmol g^{-1} per day;[39] equivalent to about 4 nmol g^{-1} h^{-1}. The accumulation rates of Ag NPs are also broadly in the nanomolar range in rainbow trout gut cell lines.[20]

Notably, the amount of total Ag accumulated by the gut from exposure to Ag_2S NPs was much higher in the mucosa of the mid intestine than any other treatment (Table 2) and with the highest accumulation rate (12 nmol g^{-1} h^{-1}, Table 3). This suggests that the mucosa of the mid intestine has a particular affinity for Ag from Ag_2S. The reason for this observation requires further investigation, but it could imply that the uptake pathways for Ag NPs and Ag_2S are different in this region of the gut. Khan *et al.*[40] found both amantadine- and nystatin-dependent uptake of Ag NPs in estuarine snails, suggesting that at least two pathways may exist (clathrin- and caveolae-mediated endocytosis, respectively). The pyloric caeca of the anterior intestine also had high silver concentrations, leading to them containing an estimated 30–54% of the silver dose (Table 4). However, this data is not interpreted as substantial internal uptake of total Ag (form unknown) into the mucosa. The pyloric caeca are extremely difficult to dissect open and separate from the surrounding mesentery. The high values for the caeca are therefore likely an artefact of Ag that could not be washed from the lumen in this portion of the gut. Dietary metal concentrations in the anterior intestine that include the pyloric tissue are rarely reported, but the values with the pyloric caeca included tend to be higher than those in the mid intestine *in vivo* (*e.g.* copper,[41]), and likely for the same reasons of difficulty in washing excess metal out of the caeca.

Some metal accumulation is also reported in the muscularis, regardless of the type of silver exposure (Table 2), which represents 1–2% of the dose (Table 4). In this experiment, the muscularis is essentially all the tissue remaining after the mucosa has been stripped from the surface and will therefore include blood vessels and the lymphatics. For dissolved silver, the measured total Ag in the muscularis may therefore represent ions that have been exported from the mucosal cells into the serosal side (*i.e.*, into the capillaries) or Ag^+ ions that have permeated into the muscularis *via* a paracellular route through the mucosa. The latter is unlikely given that net water fluxes are often in the opposite direction, but active export from the mucosal cell into the blood against the electrochemical gradient is regarded as the rate-limiting step in trace metal uptake.[42] The presence of some total Ag in the muscularis from the Ag NP and Ag_2S NP exposures needs further investigation, but might imply vesicular serosal export of Ag from the epithelial cells, as is known for Cu.[21]

Conclusions and regulatory perspective

In conclusion, the gut sac technique has been used for decades to investigate the dietary bioavailability of the dissolved metals including silver, and here the method is demonstrated for two different types of silver-containing ENMs. The data show that both dissolved and nano forms of Ag have limited bioavailability to the gut mucosa, with only a few percent of the dose being accumulated in the epithelium and even less being transferred to the serosal side. This might predict a modest or negligible bioaccumulation potential *in vivo*. In the present study, Ag from $AgNO_3$ was accumulated more than the equivalent nano forms, with only a

couple of exceptions. Therefore, from a regulatory toxicology perspective, the existing data sets on dissolved silver should be protective of the nano forms. The gut sac method has utility as a screening tool to identify materials of concern as well as the anatomical regions of the gut involved in uptake. A tiered approach for the measurement of the bioaccumulation potential of ENMs has already been proposed,[8] and the current data add to the weight of evidence that the *ex vivo* gut sac approach can be used to reduce the burden of regulatory work as well as the use of animals for *in vivo* testing.

Conflicts of interest

There are no conflicts of interest.

Acknowledgements

This work was supported by the EU H2020 NanoFase project, grant agreement No 646002. The authors would like to thank Ben Eynon for assistance with fish husbandry, and Andrew Atfield and Dr Will Vevers for technical support. Additionally, we thank Dr Rob Clough and Dr Andrew Fisher for help with ICP-MS.

References

1 J. Fabrega, S. N. Luoma, C. R. Tyler, T. S. Galloway and J. R. Lead, Silver nanoparticles: behaviour and effects in the aquatic environment, *Environ. Int.*, 2011, **37**, 517–531.
2 G. V. Lowry, K. B. Gregory, S. C. Apte and J. R. Lead, Transformations of nanomaterials in the environment, *Environ. Sci. Technol.*, 2012, **46**, 6893–6899.
3 C. Levard, E. M. Hotze, G. V. Lowry and G. E. Brown Jr, Environmental transformations of silver nanoparticles: impact on stability and toxicity, *Environ. Sci. Technol.*, 2012, **46**, 6900–6914.
4 J. R. Lead, G. E. Batley, P. J. Alvarez, M. N. Croteau, R. D. Handy, M. J. McLaughlin, J. D. Judy and K. Schirmer, Nanomaterials in the environment: behavior, fate, bioavailability, and effects — An updated review, *Environ. Toxicol. Chem.*, 2018, **37**, 2029–2063.
5 H. Ma, P. L. Williams and S. A. Diamond, Ecotoxicity of manufactured ZnO nanoparticles–a review, *Environ. Pollut.*, 2013, **172**, 76–85.
6 M. S. Khan, F. Jabeen, N. A. Qureshi, M. S. Asghar, M. Shakeel and A. Noureen, Toxicity of silver nanoparticles in fish: a critical review, *J. Biodivers. Environ. Sci.*, 2015, **6**, 211–227.
7 H. Selck, R. D. Handy, T. F. Fernandes, S. J. Klaine and E. J. Petersen, Nanomaterials in the aquatic environment: A European Union–United States perspective on the status of ecotoxicity testing, research priorities, and challenges ahead, *Environ. Toxicol. Chem.*, 2016, **35**, 1055–1067.
8 R. D. Handy, J. Ahtiainen, J. M. Navas, G. Goss, E. A. Bleeker and F. von der Kammer, Proposal for a tiered dietary bioaccumulation testing strategy for engineered nanomaterials using fish, *Environ. Sci.: Nano*, 2018, 2030–2046.
9 H. T. Ratte, Bioaccumulation and toxicity of silver compounds: a review, *Environ. Toxicol. Chem.*, 1999, **18**, 89–108.
10 T. Y. Sun, F. Gottschalk, K. Hungerbühler and B. Nowack, Comprehensive probabilistic modelling of environmental emissions of engineered nanomaterials, *Environ. Pollut.*, 2014, **185**, 69–76.
11 R. Kaegi, A. Voegelin, C. Ort, B. Sinnet, B. Thalmann, J. Krismer, H. Hagendorfer, M. Elumelu and E. Mueller, Fate and transformation of silver nanoparticles in urban wastewater systems, *Water Res.*, 2013, **47**, 3866–3877.
12 S. Li, L. K. Wallis, H. Ma and S. A. Diamond, Phototoxicity of TiO_2 nanoparticles to a freshwater benthic amphipod: are benthic systems at risk?, *Sci. Total Environ.*, 2014, **466**, 800–808.
13 S. J. Clearwater, A. M. Farag and J. S. Meyer, Bioavailability and toxicity of dietborne copper and zinc to fish, *Comp. Biochem. Physiol., Part C: Toxicol. Pharmacol.*, 2002, **132**, 269–313.
14 R. D. Handy, J. C. McGeer, H. E. Allen, P. E. Drevnick, J. W. Gorsuch, A. S. Green, A.-K. Lundebye-Haldorsen, S. E. Hook, D. R. Mount and W. A. Stubblefield, in *Toxicity of Dietborne Metals to Aquatic Organisms*, ed. W. J. A. J. S. Meyer, K. V. Brix, S. N. Luoma, D. R. Mount, W. A. Stubblefield and C. M. Wood, SETAC Press Pensacola, USA, 2005, pp. 59–112.
15 F. Galvez and C. M. Wood, Physiological effects of dietary silver sulfide exposure in rainbow trout, *Environ. Toxicol. Chem.*, 1999, **18**, 84–88.
16 F. Galvez, C. Hogstrand, J. C. McGeer and C. M. Wood, The physiological effects of a biologically incorporated silver diet on rainbow trout (*Oncorhynchus mykiss*), *Aquat. Toxicol.*, 2001, **55**, 95–112.
17 J. H. Bisesi Jr, J. Merten, K. Liu, A. N. Parks, A. N. Afrooz, J. B. Glenn, S. J. Klaine, A. S. Kane, N. B. Saleh and P. L. Ferguson, Tracking and quantification of single-walled carbon nanotubes in fish using near infrared fluorescence, *Environ. Sci. Technol.*, 2014, **48**, 1973–1983.
18 C. S. Ramsden, T. J. Smith, B. J. Shaw and R. D. Handy, Dietary exposure to titanium dioxide nanoparticles in rainbow trout, (*Oncorhynchus mykiss*): no effect on growth, but subtle biochemical disturbances in the brain, *Ecotoxicology*, 2009, **18**, 939–951.
19 M. Connolly, M. Fernandez, E. Conde, F. Torrent, J. M. Navas and M. L. Fernandez-Cruz, Tissue distribution of zinc and subtle oxidative stress effects after dietary administration of ZnO nanoparticles to rainbow trout, *Sci. Total Environ.*, 2016, **551**, 334–343.
20 M. Minghetti and K. Schirmer, Effect of media composition on bioavailability and toxicity of silver and silver nanoparticles in fish intestinal cells (RTgutGC), *Nanotoxicology*, 2016, **10**, 1526–1534.
21 R. D. Handy, M. M. Musonda, C. Phillips and S. J. Falla, Mechanisms of gastrointestinal copper absorption in the African walking catfish: Copper dose-effects and a novel anion-dependent pathway in the intestine, *J. Exp. Biol.*, 2000, **203**, 2365–2377.

22 N. R. Bury, M. Grosell, C. M. Wood, C. Hogstrand, R. Wilson, J. C. Rankin, M. Busk, T. Lecklin and F. B. Jensen, Intestinal iron uptake in the European flounder (*Platichthys flesus*), *J. Exp. Biol.*, 2001, **204**, 3779–3787.

23 I. Hoyle and R. D. Handy, Dose-dependent inorganic mercury absorption by isolated perfused intestine of rainbow trout, Oncorhynchus mykiss, involves both amiloride-sensitive and energy-dependent pathways, *Aquat. Toxicol.*, 2005, **72**, 147–159.

24 A. A. Ojo and C. M. Wood, In vitro characterization of cadmium and zinc uptake via the gastro-intestinal tract of the rainbow trout (*Oncorhynchus mykiss*): interactive effects and the influence of calcium, *Aquat. Toxicol.*, 2008, **89**, 55–64.

25 R. W. Kwong and S. Niyogi, The interactions of iron with other divalent metals in the intestinal tract of a freshwater teleost, rainbow trout (*Oncorhynchus mykiss*), *Comp. Biochem. Physiol., Part C: Toxicol. Pharmacol.*, 2009, **150**, 442–449.

26 A. R. Al-Jubory and R. D. Handy, Uptake of titanium from TiO_2 nanoparticle exposure in the isolated perfused intestine of rainbow trout: nystatin, vanadate and novel CO_2-sensitive components, *Nanotoxicology*, 2013, **7**, 1282–1301.

27 E. A. Ferguson and C. Hogstrand, Acute silver toxicity to seawater-acclimated rainbow trout: Influence of salinity on toxicity and silver speciation, *Environ. Toxicol. Chem.*, 1998, **17**, 589–593.

28 N. R. Bury, F. Galvez and C. M. Wood, Effects of chloride, calcium, and dissolved organic carbon on silver toxicity: Comparison between rainbow trout and fathead minnows, *Environ. Toxicol. Chem.*, 1999, **18**, 56–62.

29 A. A. Ojo and C. M. Wood, In vitro analysis of the bioavailability of six metals via the gastro-intestinal tract of the rainbow trout (*Oncorhynchus mykiss*), *Aquat. Toxicol.*, 2007, **83**, 10–23.

30 B. J. Shaw, G. Al-Bairuty and R. D. Handy, Effects of waterborne copper nanoparticles and copper sulphate on rainbow trout, (*Oncorhynchus mykiss*): Physiology and accumulation, *Aquat. Toxicol.*, 2012, **116**, 90–101.

31 C. Bucking and C. Wood, The effect of postprandial changes in pH along the gastrointestinal tract on the distribution of ions between the solid and fluid phases of chyme in rainbow trout, *Aquacult. Nutr.*, 2009, **15**, 282–296.

32 A. Besinis, T. De Peralta and R. D. Handy, The antibacterial effects of silver, titanium dioxide and silica dioxide nanoparticles compared to the dental disinfectant chlorhexidine on *Streptococcus mutans* using a suite of bioassays, *Nanotoxicology*, 2014, **8**, 1–16.

33 R. D. Handy and R. J. Maunder, in *Osmoregulation and Ion Transport: Integrating Physiological, Molecular and Environmental Aspects*, ed. R. D. Handy, N. Bury and G. Flik, Society for Experimental Biology Press, London, 2010, pp. 203–235.

34 D. S. Smith, R. A. Bell and J. R. Kramer, Metal speciation in natural waters with emphasis on reduced sulfur groups as strong metal binding sites, *Comp. Biochem. Physiol., Part C: Toxicol. Pharmacol.*, 2002, **133**, 65–74.

35 A. P. Gondikas, A. Morris, B. C. Reinsch, S. M. Marinakos, G. V. Lowry and H. Hsu-Kim, Cysteine-induced modifications of zero-valent silver nanomaterials: implications for particle surface chemistry, aggregation, dissolution, and silver speciation, *Environ. Sci. Technol.*, 2012, **46**, 7037–7045.

36 S. Mandal, A. Gole, N. Lala, R. Gonnade, V. Ganvir and M. Sastry, Studies on the reversible aggregation of cysteine-capped colloidal silver particles interconnected via hydrogen bonds, *Langmuir*, 2001, **17**, 6262–6268.

37 N. R. Bury and C. M. Wood, Mechanism of branchial apical silver uptake by rainbow trout is via the proton-coupled Na^+ channel, *Am. J. Physiol.*, 1999, **277**, R1385–R1391.

38 K. Shephard, The influence of mucus on the diffusion of chloride ions across the oesophagus of the minnow (*Phoxinus phoxinus* L.), *J. Physiol.*, 1984, **346**, 449–460.

39 F. R. Khan, S. K. Misra, J. Garcia-Alonso, B. D. Smith, S. Strekopytov, P. S. Rainbow, S. N. Luoma and E. Valsami-Jones, Bioaccumulation dynamics and modeling in an estuarine invertebrate following aqueous exposure to nanosized and dissolved silver, *Environ. Sci. Technol.*, 2012, **46**, 7621–7628.

40 F. R. Khan, S. K. Misra, N. R. Bury, B. D. Smith, P. S. Rainbow, S. N. Luoma and E. Valsami-Jones, Inhibition of potential uptake pathways for silver nanoparticles in the estuarine snail Peringia ulvae, *Nanotoxicology*, 2015, **9**, 493–501.

41 C. Kamunde and C. M. Wood, The influence of ration size on copper homeostasis during sublethal dietary copper exposure in juvenile rainbow trout, *Oncorhynchus mykiss*, *Aquat. Toxicol.*, 2003, **62**, 235–254.

42 R. D. Handy and F. B. Eddy, in *Physicochemical Kinetics and Transport at Chemical-Biological Interphases*, ed. H. P. v. L. W. Köster, John Wiley, Chichester, 2004, pp. 337–356.

